Master thesis

Synthesis and characterization of transition metal carbonyl clusters with chiral ligands and their application in asymmetric catalysis

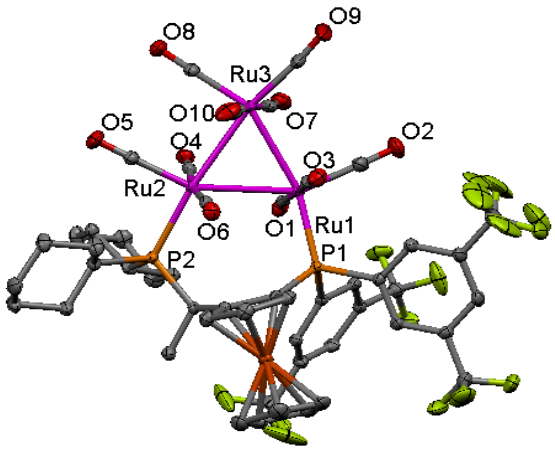

Atef Mahmoud Bakr Manaa

Lund University
Chemical Physics department

Supervisor: Professor Ebbe Nordlander
Co-advisor: Dr. Abdul Mottalib

Contents

1.Abstract

Triruthenium dodecacarbonyl was reacted with the non chiral ligand PSSP as well as chiral ferrocenyl diphosphines of the Josiphos (J008, J006 and J015) and Walphos (W009) families to give $[Ru_3(CO)_{10}(\mu\text{-}1,2\text{-P-P})]$, (P-P = W009 **1**, J008 **2**, J006 **3**, J015 **4** and PSSP **5**. The X-ray structure of **3** shows that a Ru-Ru edge is bridged by a diphosphine ligand in an equatorial coordination mode. The corresponding clusters with the ligand in a chelating coordination mode were also obtained as minor products. The tetraruthenium cluster $[H_2Ru_4(CO)_{13}]$ was reacted with chiral diphosphine ligands of the Josiphos family (J007 and J015). Four products were isolated: $[H_2Ru_4(CO)_{11}(\mu\text{-}1,2\text{-J007})]$ **6** and $[H_2Ru_4(CO)_{11}(\mu\text{-}1,2\text{-J015})]$ **7**, in which the diphosphine coordinates in a bridging mode, as well as $[H_2Ru_4(CO)_{11}(\mu\text{-}1,1\text{-J007})]$ **8** and $[H_2Ru_4(CO)_{11}(\mu\text{-}1,1\text{-J015})]$ **9**, where the diphosphine coordinates in a chelating mode. Clusters **6** and **7** were found to give high conversion and good enantiomeric excess for the hydrogenation of tiglic acid. IR spectroscopy indicates that **6** is a precursor to the active catalyst, while **8** may be an active catalyst.

2- Introduction

2.1. Classification of metal clusters

Clusters may be classified into three groups. The first group is the clusters of the early transition metals such as Cr or Sc, which are bonded by π-donor ligands (e.g. X^-, O^{2-}; X= halide). The second group is the clusters of the late transiton metals (e.g. Ru, Cu) which are bonded by π-acceptor ligands such as carbon monoxide and phosphines; the metals in these clusters have very low oxidation state (0 or negative). The third group is called "naked" clusters and consists of main group metals, e.g. $[Pb5]^{2-}$. The research described in this concerned with ruthenium clusters that belong to the second group.

2.2. The triruthenium cluster

The triruthenium cluster $[Ru_3(CO)_{12}]$ has a triangular metal center with four terminal carbonyl ligands attached to each ruthenium atom, two in axial and two in equatorial positions (Fig. 1).

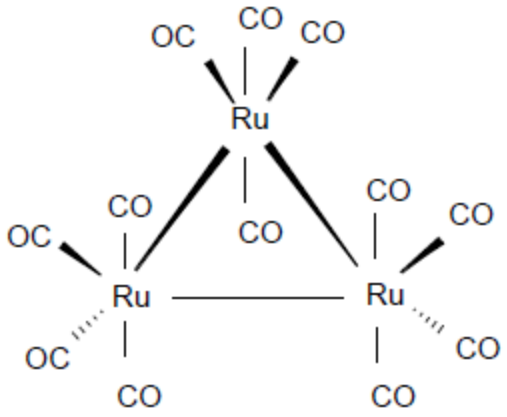

Figure 1. Triruthenium dodecacarbonyl clusteter.

Figure 1. Schematic structure of the triruthenium dococacarbonyl cluster.

There are two types of bonding interaction between the metal atom and carbon monoxide. There is a σ-bond - donation of a lone pair of electrons from the carbon monoxide to an empty d-orbital of the metal atom. The second type of bonding interaction is a π-bond, donation of electrons from the filled d-orbitals of the metal atom to the antibonding orbitals of carbon monoxide. Both binding interactions occur at the same time, and one reinforces the other [2] (Fig. 2).

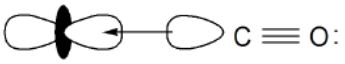

Figure 2a. σ donation

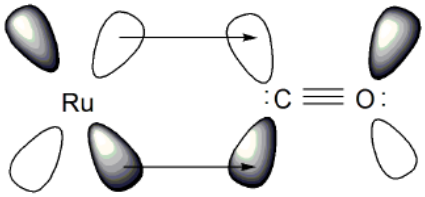

Figure 2b. π Back bonding

The diphosphine derivatives of triruthenium dodecacarbonyl clusters have been extensively studied, and some of them have been used as catalysts in hydrogenation, hydroformylation[3] and isomerisation reactions.

2.3. The tetraruthenium cluster

The tetraruthenium carbonyl hydride cluster $[H_2Ru_4(CO)_{13}]$ (see below) is prepared from $[Ru_3(CO)_{12}]$ under a variety of conditions including reduction with $NaBH_4$ in THF, treatment with OH^- in methanol followed by acidification, reflux in various solvents and reaction with alcohols, aldehydes and ketones.[4]

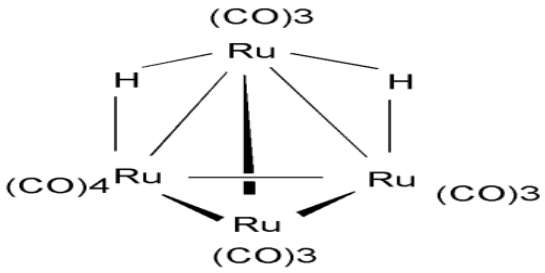

Figure 3. Schematic representation of the tetraruthenium carbonyl hydride cluster $[H_2Ru_4(CO)_{13}]$

The diphosphine derivatives of tetraruthenium cacarbonyl hydride clusters have been successfully studied, and many of them have been used as catalysts and catalyst precursors in hydrogenation, hydroformylation and isomerisation reactions. The same types of coordination modes of the diphosphines are found as for the triruthenium dodecarbonyl cluster (see below).

2.4. Chiral ferrocenyl-based phosphine ligands

The carbon monoxide ligands in the transition metal clusters are easily replaced by phosphine ligands[5] (see below). The phosphines may coordinate in axial or equatorial positions or both. Chiral ferrocenyl phosphine ligands from the Josiphos and Walphos families were used in this research. They show central and planar chirality. The central chirality is placed in the ligand backbone[6,7] (Fig. 4) and the planar chirality is resulting from asymmetric substitution of the ferrocenyl unit.

4

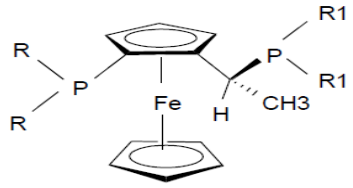

Figure 3a. Structure of Josiphos ligands

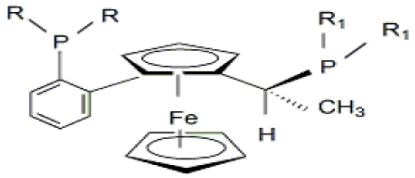

Figure 3b. Structure of Walphos ligands

4a)

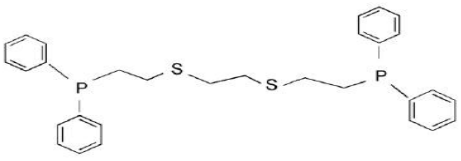

PSSP

(R)-(S)-Josiphos

ligand	R	R1
J008	3,5-$(CF_3)_2C_6H_5$	Xyl
J006	3,5-$(CF_3)_2C_6H_5$	Cy
J015	Xyl	Furan

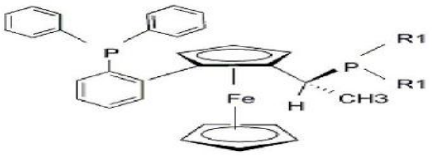

(R)-(R)-Walphos

ligand	R	R1
W009	Xyl	Xyl

4b)

"Figure 4a" and "Figure 4b" . General structures of the diphosphine ligands used in this study.

2.5. Methods of ligand substitution reactions on carbonyl clusters

In this study, a number of diphosphine-substituted ruthenium carbonyl clusters have been prepared. There are a few common methods for the introduction of phosphines and related ligands in transition metal carbonyl clusters. These methods are described below.

2.5.1. Radical-ion initiated substitution mechanism

The carbonyl substitution may be initiated by the diphenyl ketyl radical. The radical catalysed mechanism has not been resolved until now but suggestions have been made by Simpson et al. and Bruce et al[10] (see equations 1,2 and 3). They suggested electron transfer from the diphenyl ketyl radical to triruthenium dodecacarbonyl followed by nucleophilic attack of the incoming ligand (L).

$$Ru_3(CO)_{12} + [Ph_2CO]^{\cdot-} \longrightarrow [Ru_3(CO)_{12}]^{\cdot-} + Ph_2CO \quad (1)$$

$$[Ru_3(CO)_{12}]^{\cdot-} + (L) \longrightarrow [Ru_3(CO)_{11}L]^{\cdot-} + CO \quad (2)$$

$$[Ru_3(CO)_{11}L]^{\cdot-} + Ru_3(CO)_{12} \longrightarrow [Ru_3(CO)_{11}L] + [Ru_3(CO)_{12}]^{\cdot-} \quad (3)$$

2.5.2. Thermal substitution reaction.

This substitution reaction has a good effect on the replacement of the carbonyl ligands. The carbonyl ligand can be replaced thermally by heating or radiation (see eq 4). After M-CO cleavage, the metal has a vacant coordination site and a deficiency of two valence electrons, giving high reactivity. The incoming ligand can bind or attack the cluster resulting in a substituted metal carbonyl cluster[11] (see equation 5)

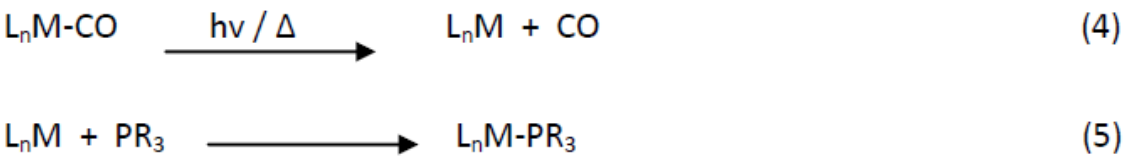

2.5.3 Oxidative decarbonylation.

In the oxidative decarbonylation reaction, trimethylamine N-oxide is used as a decarbonylation reagent. This reaction occurs via an associative mechanism (I_a). The trimethylamine N-oxide coordinates to M with CO ligands. The carbon dioxide will be lost and an unstable complex will be formed (see eq 6). The desired phosphine will replace the Me_3N ligand[12] to form the expected product (see eq 7).

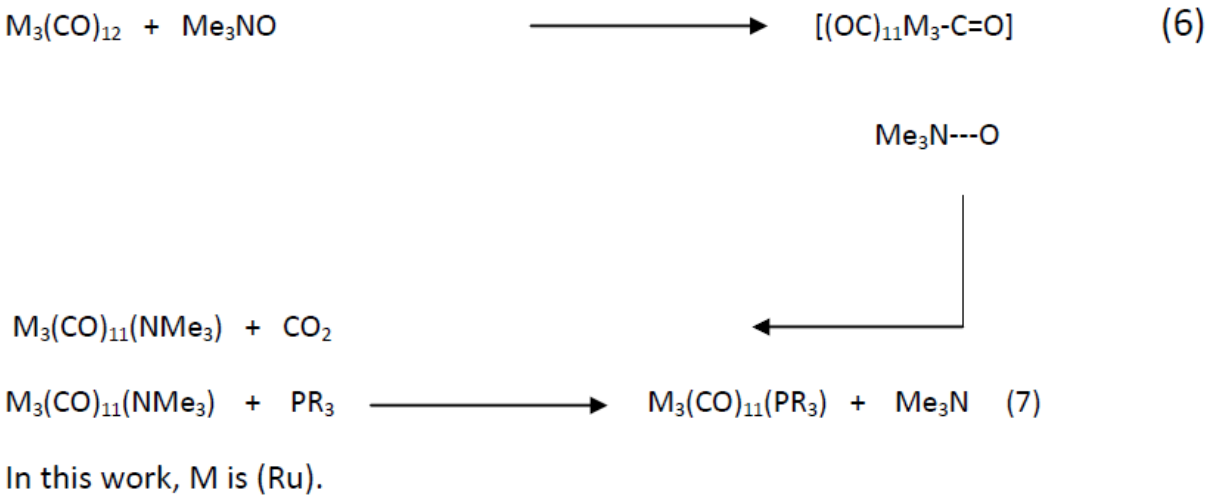

2.6. Clusters as homogeneous catalysts

Transition metal carbonyl clusters are known to be able to catalyze many organic reactions. They work as homogeneous catalysts or catalyst precursors in catalytic hydrogenation, hydroformylation[8] and isomerisation[9] reactions. In this work, a number of chiral diphosphine substituted tri- and tetranuclear clusters have been prepared and the potential of two of these clusters to act as catalysts for asymmetric hydrogenation has been investigated.

3. Experimental

General. All reactions and routine manipulations were carried out under inert atmosphere (nitrogen). The reactions were performed at room temperatures unless otherwise noted (22^{o}C). All solvents used in syntheses, catalysis and esterifications were dried prior to use. ^{1}H-NMR, ^{31}P-NMR spectra were recorded on a Varian Inova 500 MHz spectrometer using deuterated solvent ($CHCl_3$). ^{31}P-NMR shifts were referenced to external H_3PO_4. Infra-red spectra were recorded on a Nicolet Avatar 360 FT-IR. Fast Atom Bombardment mass spectra obtained also were recorded the same. Thin-layer chromatography was performed on commercially available 20 x 20 cm glass plates, covered with Merk Kieselgel 60 to 0.25 mm thickness. The chiral phosphines were enantiomerically pure samples that were obtained from Solvias AG. The parent tetraruthenium cluster [$H_2Ru_4(CO)_{13}$] was synthesized according to the literature method.[13] The diphenyl ketyl radical was prepared by addition of 24 ml of highly dried THF to benzophenone (1.30 mmol, 236 mg) in a 100 ml Schlenk tube, and subsequent addition of small pieces of sodium (1.35 g) under effect of vigorous stirring during a period of 2 h. The color of the solution changed from green over dark blue to violet and the concentration of Na[Ph_2CO] was estimated to be 0.057 mol/l.

3.1. Preparation of [$Ru_3(CO)_{10}$(PSSP)] (5)

To a mixture of 8 ml of acetonitrile (MeCN) and 30 ml of dichloromethane, [$Ru_3(CO)_{12}$] (100 mg, 0,156 mmol) and trimethylamine oxide (Me_3NO) (12 mg, 0,156 mmol) were added under nitrogen and with vigorous stirring. The temperature was reduced to –78 ^{o}C by putting the mixture in dry ice with acetone. The ligand PSSP 1,2 bis(2-diphenylphosphino)ethylthio)ethane (97 mg, 0,187 mmol). Me_3NO was added drop by drop and the color changed from yellow to red (within 60 min). The dry ice was removed after 1.5 h and the ligand PSSP (97 mg, 0,187 mmol) was added then 15 ml of dichloromethane were added drop by drop to the mixture through the adaptor. The reaction was stopped after one additional hour, then the solvent was removed *in vacuo*. Separation by TLC using n-hexane/dichloromethane (1:1 v/v) as eluent gave two bands: the minor band was yellow which was the starting material (unreacted [$Ru_3(CO)_{12}$]), and red band which is the main product [$Ru_3(CO)_{10}$(μ-1,2-PSSP] **5**, the red band was collected in

dichloromethane, the solvent was evaporated and the red product $[Ru_3(CO)_{10}(\mu\text{-}1,2\text{-PSSP}]$ **5** (2 mg, 0,015 mmol, 11.5%) was analyzed by IR, ^{1}H-NMR, ^{31}P-NMR, MS and crystallization was done in hexane/dichloromethane in a small flask and the crystals have not analyzed until now.

$[Ru_3(CO)_{10}(\mu\text{-}1,2\text{- PSSP})]$ **5**, IRυ_{CO}/cm^{-1}, CH_2Cl_2] : 2075s, 2016vs, 2009w, 1993vs, 1973vw. ^{1}H-NMR, ($CDCl_3$, at 298K), (500 MHz*),* δ= 2.88 (m, 4H), δ= 2.46 (m, 4H), δ= 2.36 (m, 4H), δ= 7.43-7.71 (m, 20H). ^{31}P[^{1}H] NMR, ($CDCl_3$, at 298K), δ =28.44(s) ppm. MS [FAB+] 1105 [M+].

3.2. Preparation of $[Ru_3(CO)_{10}(\mu\text{-}1,2\text{-W009})]$ (1)

To a dry tetrahydrofuran THF solution (6 ml), $[Ru_3(CO)_{12}]$ (15 mg, 23 mmol) and W009 (R)- 1-[(R)- 2 -(2´-Di-(3,5-xylyl) – phosphenophenyl)ferrocenyl]ethyldi(3,5-xylyl)phosphine (18 mg, 23 mmol) were added in a Schlenk tube under nitrogen pressure and the reaction mixture was heated at 70^{o}C. The color of the reaction mixture changed from yellow to dark red within 10 min. The reaction was monitored by TLC and no study material was found after 9 hours. The solvent was removed in *vacuo* and the residue was separated by TLC on silica gel. Elution with hexane/CH_2Cl_2 (7:3; v/v) gave three bands. The first moving band gave unconsumed starting material $[Ru_3(CO)_{12}]$. The second band which was major yielded $[Ru_3(CO)_{10}(\mu\text{-}1,2\text{-W009}]$ **1** (8 mg, 12.5 mmol, 25%) as red solid which was analyzed by IR υ_{CO}, ^{1}H-NMR, ^{31}P-NMR, MS=1342 [M^+] and the third band was brown decomposed product.

$[Ru_3(CO)_{10}(\mu\text{-}1,2\text{-W009})]$ **1**, IRυ_{CO}/cm^{-1}, CH_2Cl_2] : 2066s, 2009vs, 2009vs, 1994b,s, 1963m (with shoulder at 1932). ^{1}H-NMR, ($CDCl_3$, at 298K), (500 MHz), δ= 7.84 (S, 3H, ph), δ= 7.72 (s, 3H, ph), δ= 7.58 (s, 4H, ph), δ= 4.17 (s, 1H, Cp), δ= 2.33 (s, 3H, ph-Me), δ= 2.29 (s, 3H, ph-Me), δ= 2.22 (m, 1H, CH), δ= 2.38 (s, 3H, Ph-Me), δ= 2.31 (s, 3H, ph-Me), δ= 2.11 (s, 3H, Me). ^{31}P[^{1}H] NMR, ($CDCl_3$, at 298K), δ =54.76(s) ppm and δ=53.66(s), 43.67(s) ppm, 41.98(s) ppm. MS [FAB+] 1342 [M+].

3.3. Preparation of $[Ru_3(CO)_{10}(\mu\text{ -}1,2\text{-J008})]$ (2)

This reaction and work up is identical to that for $[Ru_3(CO)_{10}(\mu\text{-}1,2\text{- W009})]$ **1**. A total of 15 mg of $[Ru_3(CO)_{12}]$ (23 mmol) and (21 mg, 23 mmol) of J008 ((R)-1-[(S)-2-(2´-Di-(3,5-bis(trifluro-

methyl)phenyl)phosphino)-ferrocenyl]ethyldi(3,5-xylyl)phosphine) were reacted to give, in order of describing R_f, unreacted $[Ru_3(CO)_{12}]$ and $[Ru_3(CO)_{10}(\mu\text{-}1,2\text{-J008}]$ **2** (9 mg, 14 mmol, 26%) as a red solid and a third brown band (decomposed product). The crystal structure of $[Ru_3(CO)_{10}(\mu\text{-}1,2\text{-J008}]$ **2** has been solved by X-ray crystallography (see below).

$[Ru_3(CO)_{10}(\mu\text{-}1,2\text{- J008})]$ **2**, IRυ_{CO}/cm^{-1}, CH_2Cl_2] : 2078s, 2035w, 2002sh, vs, 1948w. ^{1}H-NMR, ($CDCl_3$, at 298K), (500 MHz*)*, δ= 4.56 (s, 1H, Cp), δ= 4.50 (s, 1H, Cp), δ= 4.09 (s, 5H, Cp), δ= 43.94 (s, 1H, Cp), δ= 2.41 (s, 3H, ph-Me), δ= 2.37 (s, 3H, ph-Me), δ= 2.19 (m, 1H, CH), δ= 2.12 (s, 3H, Me). ^{31}P[^{1}H] NMR, ($CDCl_3$, at 298K), δ =63.69(s) ppm and 39.86(s) ppm. MS [FAB+] 1493 [M+].

3.4. Preparation of [$Ru_3(CO)_{10}(\mu\text{-}1,2\text{-J006})$] (3)

This reaction and work up is identical to that for $[Ru_3(CO)_{10}(\mu\text{-}1,2\text{-W009})]$ **1**. A total of 13 mg of $[Ru_3(CO)_{12}]$ (20.3 mmol) and 17.6 mg (20.3 mmol) of J006, (R)-1-[(S)-2-(2´-Di-(3,5-bis(trifluro-methyl)phenyl)phosphino)-ferrocenyl]ethyldicyclohexylphosphine were reacted to give, in order of describing R_f, unreacted $[Ru_3(CO)_{12}]$ and $[Ru_3(CO)_{10}(\mu\text{-}1,2\text{-J006}]$ **3** (9 mg, 14 mmol, 30.5%) as a red solid and a third band consisting of brown decomposed product .

$[Ru_3(CO)_{10}(\mu\text{-}1,2\text{- J006})]$ **3**, IRυ_{CO}/cm^{-1}, CH_2Cl_2] : 2087s, 2059w, 2002sh, vs, 1948w. ^{1}H-NMR, ($CDCl_3$, at 298K), (500 MHz*)*, δ= 8.52 (d, J= 12.5, 3H, ph), δ= 7.98 (d, J= 12.5, 3H, ph), δ= 4.20 (s, 1H, Cp), δ= 4.10 (s, 1H, Cp), δ= 3.98 (s, 5H, Cp), δ= 3.54 (s, 1H, Cp), δ= 1.98-0.91 (m, 22H, Cy), δ= 2.25 (m, 1H, CH), δ= 2.10 (s, 3H, Me).
^{31}P[^{1}H] NMR, ($CDCl_3$, at 298K), δ =63.68(s) ppm and 39.86(s) ppm. MS [FAB+] 1451 [M+].

3.5. Preparation of [$Ru_3(CO)_{10}(\mu\text{-}1,2\text{-J015})$] (4)

This reaction and work up is identical to that for $[Ru_3(CO)_{10}(\mu\text{-}1,2\text{- W009})]$ **1**. A total of (15 mg, 23 mmol) and (14.5 mg, 23 mmol) of J015 (R)-1-[(S)-2-(2´-Di-(2-furyl)phosphino)-ferrocenyl]ethyldi(3,5-xylyl)phosphine were reacted to give, in order of decreasing R_f, unreacted $[Ru_3(CO)_{12}]$ and $[Ru_3(CO)_{10}(\mu\text{-}1,2\text{-J015}]$ **4** (7 mg, 11 mmol, 25%) as a red solid which was

analyzed by IR, ^{1}H-NMR, ^{31}P-NMR, MS=1202 [M^{+}] and the third band was brown decomposed product.

[$Ru_3(CO)_{10}$(μ-1,2-J015)] **4**, IRυ_{CO}/cm^{-1}, CH_2Cl_2] : 2076s, 2057w, 2033sh, w, 2007sh, vs, 1999sh, s, 1977w, 1960, 1697sh,s. ^{1}H-NMR, ($CDCl_3$, at 298K), (500 MHz), δ= 7.45 (s, 3H, Ph) , δ= 4.48 (s, 1H, Cp), δ= 4.35 (s, 1H, Cp), δ= 4.15 (s, 5H, Cp), δ= 3.61 (s, 1H, Cp), δ= 2.15 (s, 3H, Me), δ= 2.28 (m,1H, CH), δ= 2.54 (s, 3H, Ph-Me), δ= 1.51 (m, 8H,furan).
^{31}P[^{1}H] NMR, ($CDCl_3$, at 298K), δ =55.02(s) ppm and 5.71(s) ppm. MS [FAB+] 1202 [M+].

3.6. Synthesis of [$H_2Ru_4(CO)_{13}$] derivatives using Josiphos diphosphine ligands

3.6.1. Reaction of [$H_2Ru_4(CO)_{13}$] with J007.

[$H_2Ru_4(CO)_{13}$] (0.026 mmol, 20 mg) and J007 ((R)-1-[(S)-2-di-(4-methoxy-3,5-dimethylphenyl)phosphino)-ferrocenyl]ethyldicyclohexylphosphine) (0.034 mmol, 21 mg) were added to a 100 ml three-necked round bottom flask and dissolved in 20 ml of dichloromethane (CH_2Cl_2) and stirred at room temperature. A slight excess of Me_3NO (0.080 mmol, 6 mg) dissolved in 5 ml of dichloromethane was added drop by drop, resulting in a color change from orange to red. The reaction mixture was left under vigorous stirring for 11 hours at room temperature giving a dark red colour. The solvent was evaporated *in vacuo*. The deep red solid was dissolved in a small volume of dichloromethane and purified by preparative TLC using dichloromethane/hexane as eluent (1:1 v:v). Two well separated bands were developed, the first moving band afforded [$H_2Ru_4(CO)_{11}$(μ-1,1- J007)] **8** (3.5 mg, 9.3%) as red microcrystals while the second band gave [$H_2Ru_4(CO)_{11}$(μ-1,2- J007)] **6** (7 mg, 18.8%) as yellow crystals after crystallization from hexane/CH_2Cl_2 at -20 ^{o}C.

[$H_2Ru_4(CO)_{11}$(μ-1,2-J007)] **6**, IRυ_{CO}/cm^{-1}, CH_2Cl_2] : 2067s, 2026vs, 2009vs, 1997w, 1963w. ^{1}H-NMR, ($CDCl_3$, at 298K), *(500 MHz),* δ= 4.38 (S, 1H, Cp), δ= 4.12 (s, 5H, C_p), δ= 3.64 (s, 1H, C_p), δ= 4.12 (s, 5H, C_p), δ= 0.89-2.00 (m, 22H, C_y), δ= 2.48 (s, 3H, Ph-Me), δ= 2.39 (s, 3H, Ph-Me), δ= 3.81 (s, 3H, MeO), δ= 3.80 (S, 3H, MeO), δ= 7.78 (d, J=12.4, 2H, Ph), δ= 7.56 (d, J=12.4 , 2H, Ph), δ= 2.11(s, 3H, Me), δ= 2.24 (m, 1H, CH).

δ for hydride signals-5.0 ppm (s) -6.1 ppm(m). $^{31}P[^{1}H]$ NMR, ($CDCl_3$, at 298K), δ =27.87 ppm and δ=51.42 ppm. MS [FAB+]: 1424 [M+].

$[H_2Ru_4(CO)_{11}(1,1\text{-J007})]$ **8**, IR [υ_{CO}/cm^{-1}, CH_2Cl_2] : 2070vw, 2052s, 2027s, 1997w, 1972VS, 1933W. 1H-NMR, (CDCl3, at 298K), (500 MHz) δ= 4.39 (s, 1H, CP), δ= 4.12 (s, 5H, C_p), δ= 3.65 (s, 1H, C_p), δ= 4.15 (s, 5H, C_P), δ= 0.88-2.00 (m, 22H, C_y), δ= 2.48 (s, 3H, Ph-Me), δ= 2.43 (s, 3H, Ph-Me), δ= 3.82 (s, 3H, MeO), δ= 3.84 (s, 3H, MeO), δ= 7.79 (d, J=12.4, 2H, Ph), δ= 7.59 (d, J=12.4 , 2H, Ph), δ= 2.10 (s, 3H, Me), δ= 2.26 (m, 1H, CH).
δ for hydride signals-3.5 ppm (s) -13.3 ppm(m). $^{31}P[^{1}H]$ NMR (Fig. 10), (CDCl3, at 298K), δ =63.41 ppm and δ=34.99 ppm. MS [FAB+]: 1424 [M+].

3.6.2. Reaction of of $[H_2Ru_4(CO)_{13}]$ with J015.

A total of $[H_2Ru_4(CO)_{13}]$ (0.021 mmol, 16 mg) and J015 ((S)-1-[(R)-2-di-(2-furylphosphino) ferrocenyl]ethyldi-3,5-xylyl-phosphine (0.027 mmol, 16.7 mg) were added to a 100 ml three-necked round bottom flask, dissolved in 20 ml of dichloromethane and stirred at room temperature. A slight excess of Me_3NO (0.078 mmol, 5.8 mg) dissolved in 4 ml of dichloromethane was added drop by drop to the reaction mixture. The reaction mixture was left under vigorous stirring for 11 hours at room temperature, while a colour change from yellow to dark red was observed. The solvent was evaporated *in vacuo*. The deep red solid was dissolved in a small volume of dichloromethane and separated by preparative TLC using dichloromethane/hexane (1:1 v:v) as eluent. Two bands were developed, the first moving band afforded the chelating complex $[H_2Ru_4(CO)_{11}(1,1\text{- J015})]$ **9** (2.5 mg, 8.9%) as a yellow solid and the second moving band afforded $[H_2Ru_4(CO)_{11}(\mu\text{-}1,2\text{- J015})]$ **7** (5.5 mg, 18.9%) as a red solid.

$[H_2Ru_4(CO)_{11}(\mu\text{-}1,2\text{- J015})]$ **7**, IR [υ_{CO}/cm, CH_2Cl_2] : 2052s, 2030vs, 2007s, 1980w, 1960s. 1H-NMR, (CDCl3, at 298K), *(500 MHz)* δ= 7.89 (S, 3H, Ph), δ= 4.50 (S, 1H, CP), δ= 4.32 (s, 1H, CP), δ= 4.11 (s, 5H, CP), δ= 3.63 (s, 1H, CP), δ= 2.17 (s, 3H, Me), δ= 2.30 (m, 1H, CH) δ= 2.48 (s, 3H, Ph-Me), δ= 2.31 (s, 3H, Ph-Me), δ= 1.52 (m, 8H,furan).
δ for hydride signals-5.0 ppm (s) -6.1 ppm(m). $^{31}P[^{1}H]$ NMR, ($CDCl_3$, at 298K), δ =40.42 ppm(d, J=12.1Hz).

[$H_2Ru_4(CO)_{11}$(μ 1,1- J015)] **9**, IR [υ_{CO}/cm, CH_2Cl_2] : 2069w, 2048s, 2026vs, 1997w,2004w, 1979w, 1958W. ^{1}H-NMR ($CDCl_3$, at 298K), (500 MHz) δ= 7.86 (s, 3H, Ph), δ= 4.45 (s, 1H, C_p), δ= 4.31 (s, 1H, C_p), δ= 4.14 (S, 5H, C_p), δ= 3.64 (s, 1H, C_p), δ= 2.17 (s, 3H, Me), δ= 2.32 (m, 1H, CH) δ= 2.48 (s, 3H, Ph-Me), δ= 2.31 (s, 3H, Ph-Me), δ= 1.50 (m, 8H,furan).
δ for hydride signals -3.5 ppm (s) -13.3 ppm(m). MS [FAB+] 1333 [M+].

3.7. Catalytic hydrogenation[14]

In a typical reaction, an autoclave (Carl Roth) was loaded with [$H_2Ru_4(CO)_{11}$(μ-1,2-J007)] **6** as a catalyst (7.5 mg) and substrate (52 mg) under N_2, and the degassed solvent mixture was added (3 ml EtOH and 2 ml toluene). The reaction vessel was closed and purged three times with hydrogen before final pressurizing to 45 bars. The reaction mixture was continuously stirred with a magnetic stirrer (ca. 500 rpm) and heated at 100 ^{o}C for 32 hrs. After a cooling period of approx. 30 min., the reaction vessel was carefully depressurized and opened. The homogeneous reaction mixture was transferred to a 50 ml flask and concentrated under vacuum. The conversions for the catalysis runs were calculated on the basis of NMR analyses.[13] To separate the carboxylic acid from the cluster, the reaction residue was dissolved in Et_2O (5ml) and the carboxylic acid was extracted with $NaHCO_3$ (sat. 3x10ml) and washed with Et_2O (2x5ml). The carboxylate was protonated with H_2SO_4 (conc., q.s) and extracted with Et_2O (3x10ml) and washed with H_2O (2x5ml) and dried over Na_2SO_4. The Et_2O was removed under vacuum yielding the carboxylic acid quantitatively. The recovered cluster was dissolved in a minimum quantity of CH_2Cl_2 and the products were separated using preparative TLC (commercial 20 x 20 cm plates covered with Merk kieselgel 60, 0.25 mm thickness) with a hexane/CH_2Cl_2 (1/1 v:v) mixture as eluent. Infrared and mass spectrometry indicated that **6** had converted to the known cluster [$H_4Ru_4(CO)_{10}$(μ-1,2-J007)][13] via loss of a carbonyl ligand/addition of H_2. Catalytic hydrogenation of tiglic acid was also carried out using [$H_2Ru_4(CO)_{11}$(μ-1,2-J015)] **7** as a catalyst/catalyst precursor using the same protocol as above. However, recovery of the cluster did not indicate the same conversion to the corresponding tetraruthenium tetrahydride cluster that was observed for **6**.

3.8 Determination of enantiomeric excess

After an extraction process, the 2-methyl butyric acid (7 mg, 0.073 mmol) was added to a 100 ml Schlenk tube and dissolved in 15 ml of dichloromethane at -10 ^{o}C using a mixture of dry ice, acetone and dist. H_2O. The 4-dimethylaminopyridine (4 mg) (***toxic***), S-(+)-methyl mandelate (12 mg, 0.073 mmol) and 1,3-dicyclohexylcarbodiimide (18 mg, 0.058) (***toxic***) were added to the carboxylic acid in solvent under nitrogen pressure and stirred for 4.5 hours. After 4.5 hours, the reaction mixture was transferred to a 100 ml round bottom flask and the solvent was removed under reduced pressure to yield an oily colorless product. The product was dissolved in dichloromethane and separated with preparative TLC (commercial 20 x 20 cm plates covered with Merck kieselgel 60) using hexane/ether (1:1 v:v) as eluent yielding two bands (R_f 0.64). The first band, containting the reduced and esterified carboxylic acid, was collected and dissolved in a mixture of hexane/ether (1:1 v/v) and separated to yield a clear colorless solution. The enantiomeric excess of the hydrogenation was determined by comparison of the yield of the two possible diastereomers of the reduced carboxylic acid, as determined by ^{1}H NMR spectroscopy.[14]

4- Results and Discussion

In this work, trinuclear ruthenium carbonyl clusters containing both non-chiral (PSSP) and chiral diphosphine ligands have been synthesized and characterized. Furthermore, a number of chiral diphosphine derivatives of $[H_2Ru_4(CO)_{13}]$ were synthesized, and the capacity of two of the resultant chiral tetranuclear clusters to act as catalysts for asymmetric hydrogenation were evaluated.

4.1. Synthesis and characterization of $[Ru_3(CO)_{12}]$ derivatives using Josiphos and Walphos diphosphine ligands.

Clusters of the general formula $[Ru_3(CO)_{10}(P\text{-}P)]$, where P-P is a chiral diphosphine ligand of the Josiphos family (J006, J008 or J015) or the Walphos family (W009) (see Fig. 4, above), were synthesized via thermal substitution (Scheme 1). The bridging diequatorial coordination mode was inferred by comparison of IR spectra of the new clusters to those of known $[Ru_3(CO)_{10}(diphosphine)]$ clusters.

Scheme 1

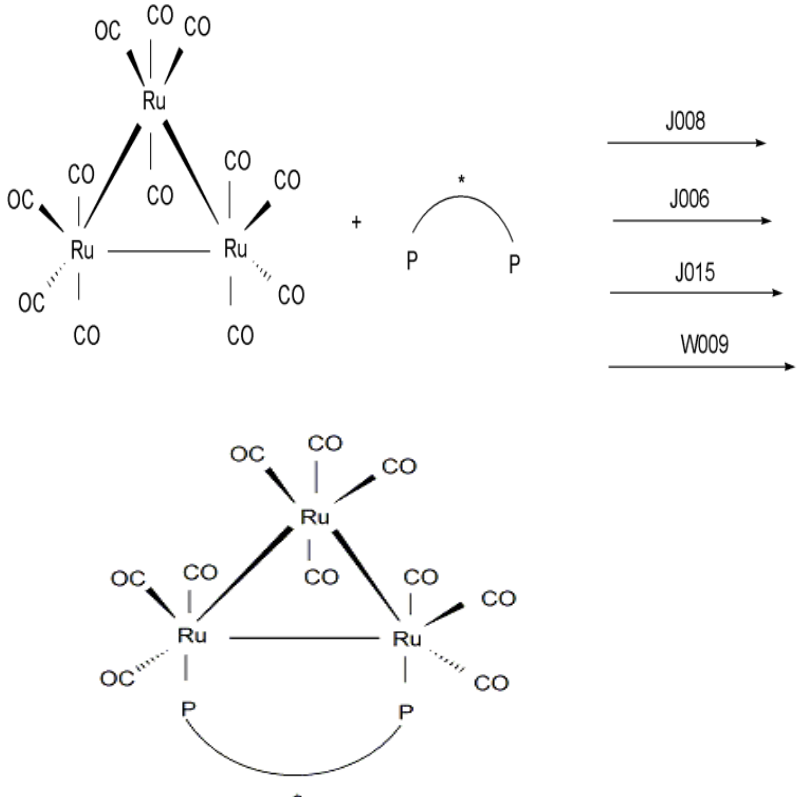

Crystals suitable for X-Ray analysis could be grown for $[Ru_3(CO)_{10}(\mu\text{-}1,2\text{-J008})]$ (**2**) and the crystal structure of **2** was determined in order to unambiguously determine the coordination mode of the diphosphine. The molecular structure of **2** is shown in Figure 5 and selected bond distances and angles are listed in Table 1. Crystallographic data for **2** are summarized in Appendix 1. The bond length average of the triruthenium core (2.873 Å) is slightly longer than what is observed for the analogous cluster $[Ru_3(CO)_{10}(\mu\text{-}1,2\text{-(dppm)}]$ (2.852 Å; dppm=bis(diphenylphosphino)methane) and other similar triruthenium clusters. However, it is surprising that the Ru-Ru-P angles reported below are essentially identical to those observed for $[Ru_3(CO)_{10}(\mu\text{-}1,2\text{-(dppm)}]$, considering that the expected bite angle of J008 should be larger than for dppm.

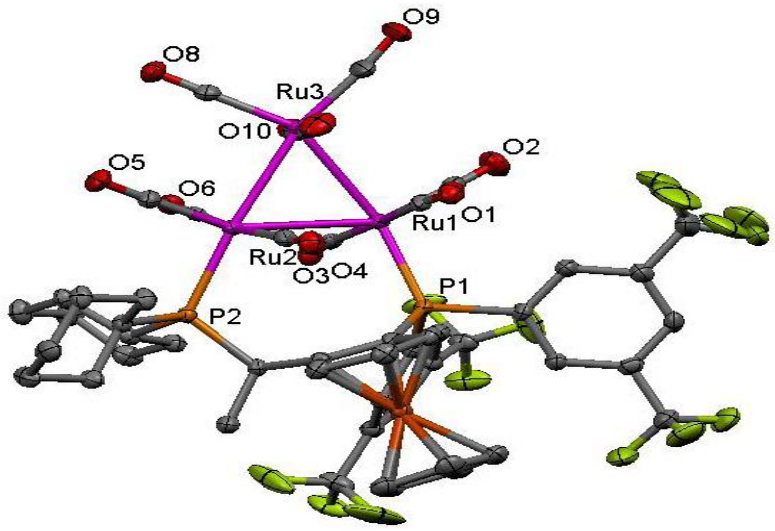

Figure 5. The molecular structure of $[Ru_3(CO)_{10}(\mu\text{-}1,2\text{-}J008)]$(**2**).

Table 1. Selected bond lengths (Å) and angels (°) for $Ru_3(CO)_{10}$(1,2-J008)

Ru(1)-Ru(2)	2.898Å	Ru(1)-P(1)	2.231Å
Ru(2)-Ru(3)	2.861Å	Ru(2)-P(2)	2.376Å
Ru(1)-Ru(3)	2.858Å		
Ru-C (carbonyl)	1.934Å		
C-O (carbonyl)	1.140Å		
Ru(1)-Ru(2)-Ru(3)	59.51°	P(1)-Ru(1)-Ru(3)	153.50Å
Ru(1)-Ru(3)-Ru(2)	60.88°	P(1)-Ru(1)-Ru(2)	99.31Å
Ru(2)-Ru(1)-Ru(3)	59.61°	P(2)-Ru(2)-Ru(3)	155.87Å
		P(2)-Ru(2)-Ru(1)	100.31Å

4.2. Synthesis and characterization of $[H_2Ru_4(CO)_{13}]$ derivatives using Josiphos ligands

Two Josiphos ligands (J007 and J015) were used to make chiral diphosphine derivatives of $[H_2Ru_4(CO)_{13}]$ (Scheme 2).

Two products were isolated in each case, the major one is bridging and the other one is the corresponding chelating complex. The major products are orange and have the formula $[H_2Ru_4(CO)_{11}(1,2\text{-P-P})]$ (P-P = J007 (**6**)**,** J015 (**7**)) and the minor are yellow $[H_2Ru_4(CO)_{11}(1,1\text{-P-P})]$ ((P-P) = J007 (**8**) or J015 (**9**)). The yields of the first (major) product were almost the same of the two ligands - 18.8% in case of the J007 ligand and 18.9% in the case of J015. The yield of the second product were also almost the same, it was 19.3% in case of using J007 ligand and 8.9% in in case of using J015 ligand. Valence electron counting rules[15] indicate that every ruthenium atom should have a formal of 18 electron but these rules do not strictly apply to larger cluster complexes; instead the electron counting rules indicate that a the overall valence electron count for a tetrahedral transition metal cluster should be 72. On this basis, two general structures for the bridging and chelating diphosphine derivatives of $[H_2Ru_4(CO)_{13}]$ can be suggested, as shown in Scheme 2.

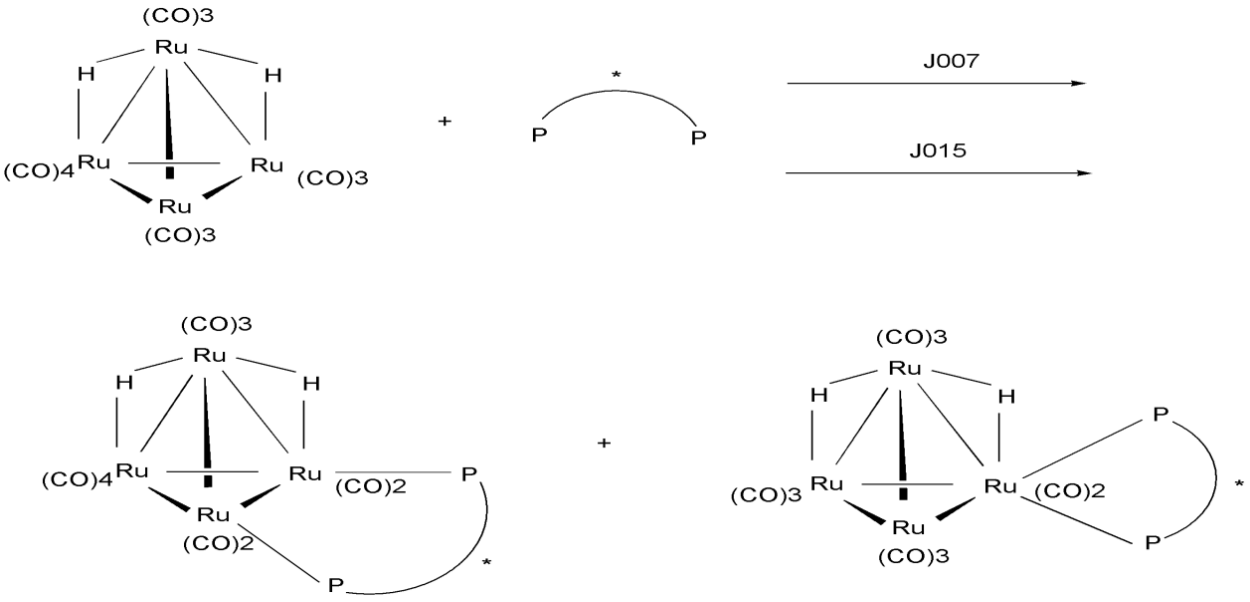

Scheme 2

4.3. Catalytic reactions

The potential of $[H_2Ru_4(CO)_{11}(1,2\text{-J007})]$ **6** and $[H_2Ru_4(CO)_{11}(1,2\text{-J015})]$ **7** to act as catalysts for the (asymmetric) hydrogenation of tiglic acid was evaluated. Two catalytic reactions have been

run using $[H_2Ru_4(CO)_{11}(1,2\text{-J007})]$ and $[H_2Ru_4(CO)_{11}(\mu\text{-}1,2\text{-J015})]$ **7** as catalysts/catalyst precursors. In the case of $[H_2Ru_4(CO)_{11}(1,2\text{-J007})]$ **6**, 73% conversion of tiglic acid to 2-methylbutyric acid was detected. It was found that $[H_2Ru_4(CO)_{11}(\mu\text{-}1,2\text{-J007})]$ **6** has been converted to $[H_4Ru_4(CO)_{10}(\mu\text{-}1,2\text{-J007})]$ during the catalytic reaction, suggesting that **6** may act as a catalyst precursor. After the catalytic reaction, the extraction process was performed in organic phase to separate the cluster from the product. After the reaction of 2-methyl butyric acid with (S) - methyl mandelate, it was obtained the product was analyzed by ^{1}H-NMR. The determination of enantiomeric excess resulted in 30%. The enantiomer R was in excess. The $[H_2Ru_4(CO)_{11}(1,2\text{-J015})]$ **7** was also used as a catalyst in the hydrogenation catalytic reaction of tiglic acid to 2-methylbutyric acid. The determination of the conversion by ^{1}H-NMR was 98%. The determination of enantiomeric excess resulted in 20% .

5- Conclusion

New trinuclear and tetranuclear ruthenium carbonyl clusters containing chiral didentate diphosphines have been successfully synthesized and characterized. The triruthenium carbonyl clusters gave clusters of the general formula $[Ru_3(CO)_{10}(\mu\text{-}1,2\text{-P-P})]$, with the diphosphine ligands coordinating in diequatorial bridging positions. The chiral tetraruthenium hydride clusters $[H_2Ru_4(CO)_{11}(1,2\text{-P-P})]$ (P-P = J007 (**6**) and J015 (**7**)) act as catalysts/catalyst precursors for asymmetric hydrogenation of tiglic acid. Good conversion of tiglic acid to 2-methylbutyric acid (73% (**6**) and 98% (**7**)) and relatively good enantioselectivey have been obtained, so other organic substrates should be tested in order to assess whether the activity depends more on the substrate or the catalyst.

Acknowledgements

First of all, I would like to thank my supervisor **Ebbe Nordlander** for all your patience, support, guidance and answering all my questions with details.

I would also like to thank

Co-advisor, **Abdul Mottalib** for his effort with me in lab.

Martin Jarenmark, for replying my questions.

Jessica Nilsson, for her help.

References

1. P.J. Dyson, J.S. McIndoe, *Transition Metal Carbonyl Cluster Chemistry*, Gordon and Breach Science Publishers, Amsterdam, 2000.
2. *Comprehensive Organometallic Chemistry II*, E.W. Abel, F.G.A. Stone, G. Wilkinson, Eds., Pergamon: Oxford, 1995.
3. E. Lozano-Diaz, A. Neels, H. Stoeckli-Evans, G. Suess-Fink, *Polyhedron*, 2001, 20, 2770-2780.
4. D.B.W. Yawne, R.J. Doedens, *Inorg. Chem*., 1972, 11, 838.
5. B. Fontal, M. Reyes, T. Suarez, F. Bellandi, J.C. Diaz, *J. Mol. Catal. A: Chem*. 1999, 149, 74-86.
6. M. Lautens, K. Fagnou, *Proc. Natl. Acad. Sci. U. S. A.* 2004, 101, 5455-5461.
7. F. Piacenti, P. Frediani, U. Matteoli, G. Menchi, M. Bianchi, *Chem. Ind. (Milan)* 1986, 68-54.
8. D.B. Berkowitz, G. Maiti, *Org. Lett*. 2004, 6, 2661-2665.
9. U. Matteoli, M. Bianchi, P. Frediani, G. Menchi, C. Botteghi, M.J. Marchetti, *J. Organomet. Chem.* 1984, 263, 243.
10. F. Piacenti, P. Frediani, U. Matteoli, G. Menchi, M. Bianchi, *Chem. Ind. (Milan)* 1986, 68-54.
11. U. Matteoli, M. Bianchi, P. Frediani, G. Menchi, C. Botteghi, M. Marchetti, *J. Organomet. Chem.* 1984, 263, 243.
12. M. I. Bruce, J. G. Matisons, B. K. Nicholson, *J. Organomet. Chem*. 1993, 275, 322.
13. V. Moberg, *Cluster-Based Catalysts for Asymmetric Synthesis*, Doctoral Thesis, Lund University, 2007, paper III.
14. E. Tyrell, M.W.H. Tsang, G.A. Skinner, J. Fawcett, *Tetrahedron*, 1996, 29, 9841.
15. J. E. Huheey, E. A. Keiter, R. L. Keiter. *Inorganic Chemistry – Principles of Structure and Reactivity*, HarperCollins College Publishers, 1993, 687.

Appendix 1. Crystallographic data for $[Ru_3(CO)_{10}(\mu\text{-}1,2\text{-}J008)]$(**2**)

Empirical formula	$C_{50}H_{40}F_{12}FeO_{10}P_2Ru_3$	
Formula weight	1449.82	
Temperature	100(2) K	
Wavelength	0.71073 Å	
Crystal system	Orthorhombic	
Space group	$P2_12_12_1$	
Unit cell dimensions	a = 13.7237(2) Å	α= 90°.
	b = 19.0556(2) Å	β= 90°.
	c = 20.0754(3) Å	γ = 90°.
Volume	5249.98(12) $Å^3$	
Z	4	
Density (calculated)	1.834 Mg/m^3	
Absorption coefficient	1.278 mm^{-1}	
F(000)	2864	
Crystal size	0.36 x 0.25 x 0.21 mm^3	
Theta range for data collection	1.47 to 30.05°.	
Index ranges	-19<=h<=19, -26<=k<=26, -28<=l<=28	
Reflections collected	122683	
Independent reflections	15338 [R(int) = 0.0440]	
Completeness to theta = 30.05°	99.8 %	
Absorption correction	Semi-empirical from equivalents	
Max. and min. transmission	0.7674 and 0.6469	
Refinement method	Full-matrix least-squares on F^2	
Data / restraints / parameters	15338 / 57 / 732	
Goodness-of-fit on F^2	1.063	
Final R indices [I>2sigma(I)]	R1 = 0.0262, wR2 = 0.0526	
R indices (all data)	R1 = 0.0335, wR2 = 0.0549	
Absolute structure parameter	-0.003(10)	
Largest diff. peak and hole	0.547 and -0.840 $e.Å^{-3}$	